analytical chemistry

pubs.acs.org/ac Article

CRISPR/Cas12a-Triggered Chemiluminescence Enhancement Biosensor for Sensitive Detection of Nucleic Acids by Introducing a Tyramide Signal Amplification Strategy

Tao Hu,* Xinxin Ke, Yangjing Ou, and Yu Lin

Cite This: *Anal. Chem.* 2022, 94, 8506−8513 Read Online

ACCESS | Metrics & More | Article Recommendations | Supporting Information

ABSTRACT: CRISPR-based biosensors have attracted increasing attention in accurate and sensitive nucleic acid detection. In this work, we report a CRISPR/Cas12a-triggered chemiluminescence enhancement biosensor for the ultrasensitive detection of nucleic acids by introducing tyramide signal amplification for the first time (termed CRICED). The hybrid chain DNA (crDNA) formed by NH_2-capture DNA (capDNA) and biotin-recognition DNA (recDNA) was preferentially attached to the magnetic beads (MBs), and the streptavidin−HRP was subsequently introduced to obtain MB@HRP-crDNA. In the presence of the DNA target, the activated CRISPR/Cas12a is capable of randomly cutting initiator DNA (intDNA) into vast short products, and thus the fractured intDNA could not trigger the toehold-mediated DNA-strand displacement reaction (TSDR) event with MB@HRP-crDNA. After the addition of tyramine−AP and H_2O_2, abundant HRP−tyramine−AP emerges through the covalent attachment of HRP−tyramine, exhibiting enhanced chemiluminescence (CL) signals or visual image readouts. By virtue of this biosensor, we achieved high sensitivity of synthetic DNA target and amplified DNA plasmid using recombinase polymerase amplification (RPA) as low as 17 pM and single-copy detection, respectively. Our proposed CRICED was further evaluated to test 20 HPV clinical samples, showing a superior sensitivity of 87.50% and specificity of 100.00%. Consequently, the CRICED platform could be an attractive means for ultrasensitive and imaging detection of nucleic acids and holds a promising strategy for the practical application of CRISPR-based diagnostics.

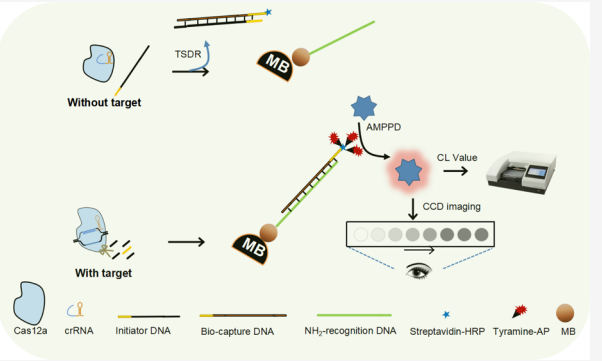

High sensitivity and specificity detection of nucleic acids is of great significance in clinical diagnosis, food safety, and environmental monitoring.[1−3] The recent advent of clustered regularly interspaced short palindromic repeat (CRISPR/Cas)-associated systems has resulted in not only remarkable awareness of gene-editing but also a revolution in molecular diagnostics tools.[4,5] Proven to possess tunable nuclease activities, a variety of innovative and powerful CRISPR/Cas-based biosensors have been proposed such as DETECTR (Cas12a),[6] SHERLOCK (Cas13a),[7] CDetection (Cas12b),[8] and Cas14-DETECTR.[9] CRISPR/Cas12a, in particular, is widely and simply applied to detection assay because it is capable of directly recognizing DNA targets by Cas12/CRISPR RNA (crRNA),[10] while the Cas13 system requires an additional transcription process for RNA recognition.[11,12] The first reported application of CRISPR/Cas12a was to employ fluorophore quencher (FQ)-labeled single-stranded DNA (ssDNA-FQ) as an output signal.[6,13,14] The activated Cas12a cleaved unrelated ssDNA-FQ without discrimination upon target recognition, leading to releasing a fluorescent signal, which can be measured by a portable method. Although optical transduction-based CRISPR/Cas12a biosensors have been useful in point-of-care, virus infection, SNP screening, and other fields,[15−17] further improvement is still necessary for broader readout modes and more practical applications.

In this regard, different types of promising CRISPR/Cas12a-based molecular diagnostic platforms have been designed according to ssDNA-labeled signal molecules or high-performance analytical instruments.[18] For example, Au nanoparticles coupled with ssDNA were introduced into the CRISPR/Cas12a-mediated colorimetric biosensors that were equipped with simple and visual readouts during the detection of nucleic acids,[19−22] while the detection sensitivity needs to be sufficiently considered. Although the CRISPR/Cas12a-based electrochemistry and electrochemiluminescence biosensors achieved high sensitivity and specificity,[23−27] they likewise suffer some defects, such as expensive electrode and

Received: April 6, 2022
Accepted: May 17, 2022
Published: May 30, 2022

https://doi.org/10.1021/acs.analchem.2c01507
Anal. Chem. 2022, 94, 8506−8513

Scheme 1. Schematic Illustration of the CRICED Platform for the Detection of Nucleic Acids

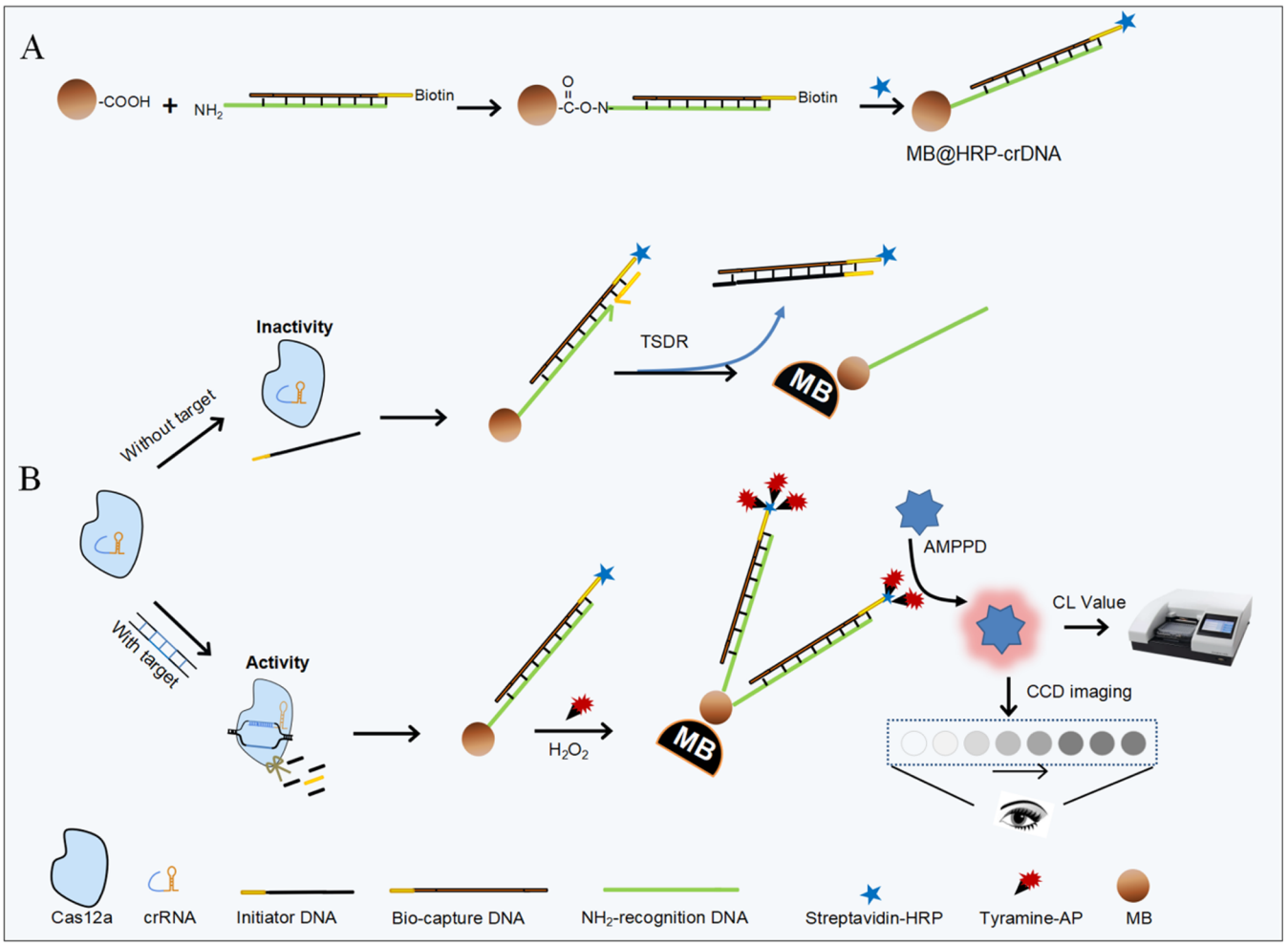

sophisticated pretreatment process, which are limited to point of care, cost-effective, and convenient detection. Hence, there is a high demand for extending the CRISPR/Cas12a system to the field of other biosensors.

Chemiluminescence (CL) has been exploited for a wide range of applications in various fields owing to its extremely high sensitivity along with other advantages, such as simple instrumentation, rapid response, and low background.[28−30] As is known to all, the typical CL signal of antibody coupled with horseradish peroxidase (HRP) and alkaline phosphatase (AP) systems have been successfully applied to commercialized immunoassay diagnosis kits.[31,32] It is noteworthy that the CL-based biosensors of DNA-strand-labeled catalytic enzymes have been employed in small molecular and nucleic acid detection and bioimaging aspects as well.[33,34] For example, the Yao group established a label-free, versatile, and low-background chemiluminescence aptasensing strategy for kanamycin.[35] The Zhao group described an aptamer structure switch assay coupled with HRP labeling on microplates for the sensitive detection of small molecules.[36] Moreover, a multiplexed CL imaging assay by integrating DNA microarray was created to screen protein biomarkers.[37] Those abovementioned DNA-strand-involved CL platforms may provide us a clue in terms of constructing a CRISPR/Cas12-based CL biosensor for the specific nucleic acid detection, where the activated Cas12a can indirectly or directly digest single-strand DNA-labeled native enzymes such as HRP and AP.

Actually, the readout of the CL signal is still subjected to limited quantum fields, and thus signal amplification is of particular interest. Tyramide signal amplification (TSA) is a robust enzyme-mediated amplification method to enhance the sensitivity in fixed-cell assays, such as immunocytochemistry and in situ hybridization.[38,39] In the presence of HRP and hydrogen peroxide (H_2O_2), tyramine allows being converted into a short-lived intermediate that rapidly and covalently binds to electron-rich regions of adjacent proteins. With the aid of convenient TSA, various immunosensors have exhibited significant sensitivity enhancement in terms of protein detection.[40−42] Recently, both the Liu group and the Yang group designed chemiluminescence imaging immunosensors based on the TSA strategy for the ultrasensitive detection of tumor biomarkers.[43,44] An ultrasensitive electrochemical immunosensor based on AuNPs-TSA for detecting procalcitonin was well-constructed.[45] To our knowledge, there are almost no reports focusing on the nucleic acid detection field with TSA. More to the point, the CRISPR/Cas12a-based biosensor by introducing TSA was not attempted.

Taking the abovementioned concepts into consideration, we established a CRISPR/Cas12a-based chemiluminescence enhancement biosensor for ultrasensitive detection of nucleic acids (CRICED) by employing tyramide signal amplification for the first time. In brief, the hybrid chain DNA (crDNA) formed by NH_2-capture DNA (capDNA) and biotin-recognition DNA (recDNA) was preferentially attached to

https://doi.org/10.1021/acs.analchem.2c01507
Anal. Chem. 2022, 94, 8506−8513

the carboxyl-coated magnetic beads (MBs), and then the streptavidin−HRP was bound to the surface of MB-crDNA (Scheme 1A). In the absence of a target (Scheme 1B), the Cas12a was not activated and the intact initiator DNA (intDNA) triggered the removal of recDNA from the assembly of MB@HRP-crDNA via a toehold-mediated DNA-strand displacement reaction (TSDR), and thus no CL signal appeared. In the presence of the target, the activated Cas12a indiscriminately cut intDNA into vast short products, thereby the HRP-labeled recDNA could not be removed by TSDR event from the as-prepared MB@HRP-crDNA. Upon the addition of tyramine−alkaline phosphatase (tyramine−AP) and H_2O_2, abundant HRP−tyramine−AP emerges through the covalent attachment of HRP−tyramine, which markedly exhibited an enhancement signal or imaging readout with a CCD camera. Our proposed CRICED platform achieved the detection sensitivity for 17 pM of synthetic DNA (stDNA) target and single copy per reaction of plasmid with the help of isothermal amplification (RPA). More importantly, the applicability of the CRICED platform was validated by testing 20 HPV clinical samples, which exhibited excellent specificity of 100% and sensitivity of 87.50% by comparison to the commercial PCR-RDB diagnosis kit, indicating huge application potential in the clinical diagnosis.

EXPERIMENTAL SECTION

Materials and Apparatus. All of the nucleic acid sequences and plasmids (Table S1) used in this study were synthesized by General Biol (Anhui) Co., Ltd (Chuzhou, China). The TwistAmp Basic kit for RPA was purchased from TwistDx Limited (U.K.). Streptavidin−HRP, streptavidin−AP, carboxyl-coated magnetic beads (MB) (20 mg/mL), and a magnetic rack were purchased from Beyotime Biotechnology (Shanghai, China). 3-[2-Spiroadamatane]-4-methoxy-4-[3-phosphoryloxy]-phenyl-1,2-dioxetane dioxetane (AMPPD) was purchased from Ji Na Bang Sheng Lifetechnology Co., Ltd. (Beijing, China). 1-Ethyl-3-(3-dimethylaminopropyl) carbodiimide (EDC) and *N*-hydroxysuccinimide (NHS) were obtained from Sigma-Aldrich. Biotin and bovine serum albumin (BSA) were supplied by Sangon Biotech (Shanghai, China). LbCas12a was purchased from Tolo Biotech (Shanghai, China). Biotin tyramine was purchased from APExBIO Technology LLC (Houston). Ultrapure water (Milli-Q synthesis, Millipore Inc., Bedford, MA) was used throughout. All of the buffer solutions were filtered and degassed before use.

The ultraviolet−visible (UV−vis) spectrum of MB@HRP-crDNA was recorded with a Hitachi UH5300 spectrophotometer (Tokyo, Japan). Chemiluminescence imaging was carried out with a bioanalytical imaging system (Syngene G: BOX F3 gel doc, U.K.). Chemiluminescence signal was measured with a BioTek Synergy H1.

Preparation of MB@HRP-crDNA. First, 4 μL of carboxyl-modified MB (MB-COOH) was washed with buffer (0.05 M MES, pH = 6.0) twice. Two microliters of EDC (50 mg/mL) and 2 μL of NHS (50 mg/mL) were incubated with MB-COOH for 0.5 h. The activated MB was washed with PBS buffer (0.02 M, pH = 7.4) three times. Meanwhile, 10 μL of NH_2-capture DNA (50 μM) and 10 μL of biotin-recognition DNA (50 μM) within 30 μL of annealing buffer were annealed by heating at 95 °C for 5 min, gradually cooling down to 25 °C at 0.1 °C/s to form crDNA. Then, 400 nM crDNA was incubated with the activated MB at room temperature for 1 h. BSA (100 μL, 1%) was next employed to block the remaining carboxyl of MB. Subsequently, 100 μL of streptavidin−HRP (1 μg/mL) was introduced into the MB-crDNA to obtain the MB@HRP-crDNA, washed twice, and stored in PBS buffer at 4 °C for further use.

Preparation of Tyramine−AP Conjugates. Ten microliters of biotin tyramine (10 mM) was incubated with 2 μL of streptavidin−AP (1 mg/mL) in 100 μL buffer (0.02 M Tris-HCl, pH = 8.0) for 0.5 h, and then 4 μL of biotin (50 mM) was introduced to block the remaining streptavidin sites. Subsequently, the resultant mixture was centrifuged (14 000*g*) for 10 min at 4 °C to remove the excess biotin tyramine and biotin twice. Finally, the tyramine−AP conjugates were suspended using 50 μL of Tris-HCl (0.02 M, pH = 8.0) and stored at 4 °C for use.

RPA Assay. An RPA kit was employed to amplify plasmids or clinical samples. According to the operating instructions, 2.4 μL of forward and reverse primers (10 μM) were added to the RPA TwistAmp Basic kit. Then, 13.2 μL of target solution was mixed. Finally, 2.5 μL of MgOAc (280 mM) was added. After incubation for 30 min at 37 °C, the obtained amplified products were stored at 4 °C before use.

Measurement of CRICED. First, the amplified products or the stDNA target was introduced into the tube containing LbCas12a-crRNA and intDNA for 30 min at 37 °C. Then, we used 5 μL of 0.2% SDS to destroy the activity of LbCas12a for 10 min. The above solution was transferred into the hole within MB@HRP-crDNA for 60 min at room temperature. After that, the coating solution was removed and washed five times using PBS buffer. Ten microliters of tyramine−AP and 2 μL of H_2O_2 (10 mM) were added to the plate for 10 min. Subsequently, the plate was rinsed thoroughly with washing buffer at least five times. Finally, 100 μL of AMPPD was introduced and incubated for 100 s. After that, the CL signal was measured with a Synergy H1 instrument and simultaneously could be observed by the naked eyes using a CCD camera.

Clinical Sample Analysis. Twenty clinical samples of HPV were kindly provided by International Peace Maternity & Child Health Hospital (Shanghai) and further confirmed with the Human Papillomavirus Genotyping Kit for 23 Types (PCR-RDB, Reverse Dot Blot) according to operating instructions. We then used the CRICED platform to test 20 clinical samples using RPA kits.

RESULTS AND DISCUSSION

Characterization of TSDR and MB@HRP-crDNA and Collateral Cleavage of intDNA. TSDR has been broadly used in the ultrasensitive detection of nucleic acids since it can be carried out at room temperature and is controllable with predictable thermodynamics and kinetics through the precise design of the sequences. To achieve highly efficient TSDR in this work, we designed three kinds of single-strand DNA (sequences listed in Table S1) according to previously reported principles.[46] Prior to TSDR, the synthetic NH_2-capDNA was partially complementary to biotin-recDNA, forming a crDNA. Expectantly, the remaining 10 bases of 5′-recDNA bound to the terminus of the intDNA under the condition of coincubation, enabling the TSDR occurrence between intDNA and crDNA, thus leading to the formation of ciDNA (recDNA and intDNA) and capDNA production. The designed sequences of TSDR were characterized and confirmed by native polyacrylamide gel electrophoresis

https://doi.org/10.1021/acs.analchem.2c01507
Anal. Chem. 2022, 94, 8506−8513

(PAGE). As illustrated in Figure 1A, lanes 1−4 showed the band of intDNA, capDNA, recDNA, and as-prepared crDNA,

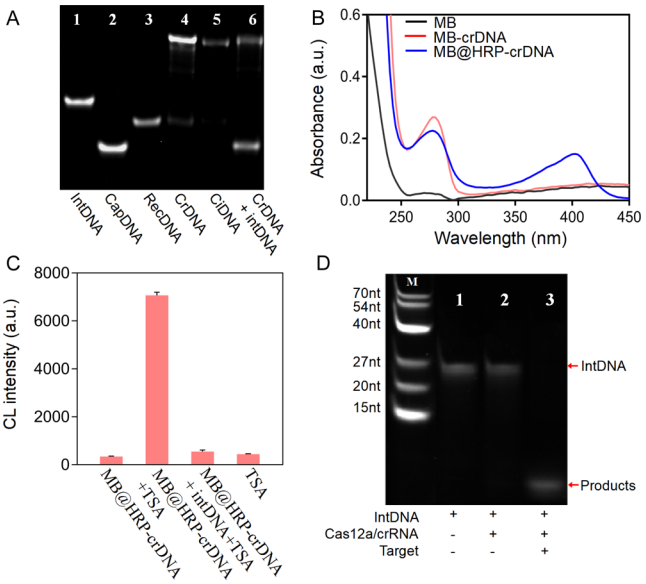

Figure 1. (A) Native PAGE analysis of the TSDR event. (B) UV−vis absorption spectrum of MB@HRP-crDNA. (C) CL responses of the MB@HRP-crDNA with TSA. (D) Denaturing PAGE characterization of collateral cleavage of intDNA (100 nM) by activated Cas12a.

respectively. Lane 6 presented the TSDR event between intDNA and as-obtained crDNA. As seen in lane 6, we found that the band of intDNA was nearly absent, whereas a distinct lower band was observed, which was consistent with the position of capDNA; meanwhile, the top band of lane 6 exhibited the same position as lane 5 containing an as-prepared ciDNA. Those results explicitly revealed that the capDNA was replaced from the crDNA by intDNA and formed a ciDNA structure at the same time, obviously suggesting that the high performance of the TSDR event was triggered by intDNA and the reasonable design of DNA sequences.

The crDNA was initially coated with MB-COOH by covalent bonding of carboxyl and amino groups in this study, where the employed MB could provide a more convenient and visual operation process by use of its magnetic properties. Subsequently, the streptavidin−HRP was effortlessly bound to the terminus of crDNA via a biotin−streptavidin manner. Figure 1B showed the typical UV−vis spectroscopy characterization of well-prepared MB@HRP-crDNA. As expected, the MB-crDNA presented an absorbance at 260 nm of DNA, whereas the MB@HRP-crDNA exhibited double absorbance at around 400 nm of HRP and 260 nm, which is in accordance with previous reports.[47] The results illustrated the successful introduction of HRP onto the MB-crDNA.

Subsequently, the performance of the TSA strategy was investigated through HRP−tyramine with the assistance of H_2O_2. As seen in Figure 1C, by comparing with MB@HRP-crDNA and TSA alone, the MB@HRP-crDNA with the TSA group showed an intense CL signal because of the formation of abundant HRP−tyramine−AP through the covalent attachment of HRP−tyramine with the help of H_2O_2, confirming that the tyramine−AP was precisely bound to MB@HRP-crDNA and efficiently catalyzed its AMPPD substrate. After the TSDR event, in addition, we discovered that the CL intensity with TSA hardly emerged as well (Figure 1C). To further explain whether the TSA is the key to enhance the CL signal, we simultaneously obtained MB@HRP-crDNA and MB@AP-crRNA. As shown in Figure S1, we figured out that the MB@HRP-crDNA with the TSA group increased approximately fourfold than the as-prepared MB@AP-crDNA under the same condition. Those results demonstrated the good feasibility and outstanding CL signal readout with the introduction of TSA.

It was reported that CRISPR/Cas12a-crRNA possessed robust collateral cleavage of ssDNA reporters containing different types of bases.[6] It is crucial to investigate whether the designed intDNA could be sheared by the activated Cas12a. We here employed human papillomavirus 16 (HPV16) as a model target for proof-of-concept. We reasonably synthesized the crRNA sequence on the basis of the L1 gene of HPV16 as well as the sense strand and antisense strand sequence for preparing the stDNA target (sequences are listed in Table S1). The PAGE analysis experiments were performed to verify the performance of the activated Cas12a for cleaving intDNA. As shown in Figure 1D, we observed that the intDNA was only digested in lane 3, which contains Cas12a, crRNA, and stDNA simultaneously. This result was indicative of the Cas12a efficiently cutting intDNA into vast short products.

Development of the CRICED Platform. To further verify the feasibility of the whole procedure by integrating the aforementioned performance, the prepared stDNA target was added to the mixture of Cas12a, crRNA, and intDNA. Once the recognition process occurred, collateral cleavage activity of Cas12a was activated, and the intDNA could be cleaved with indiscrimination. We then transferred the mixtures into the plate containing the as-prepared MB@HRP-crDNA. As shown in Figure 2A, it was surprising to find that the CL value was only observed in the presence of the stDNA target. Instead, both the control group and blank target yielded negligible CL signals. Meanwhile, the results of the proposed CRICED platform could be directly interpreted by the naked eyes through a CCD camera (Figure 2A, inset). In brief, our

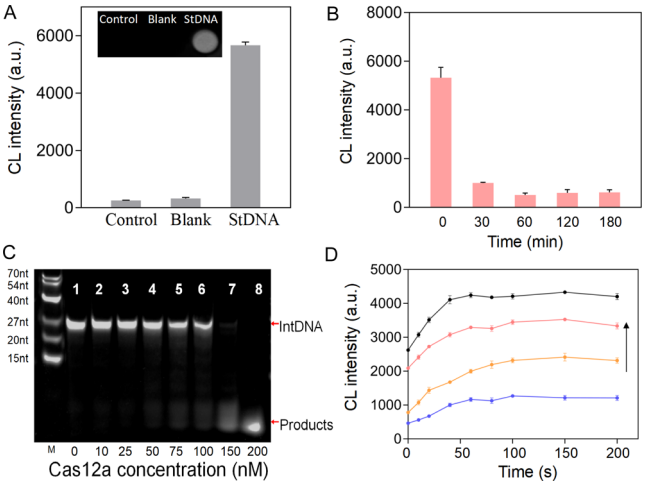

Figure 2. (A) CL responses of the feasibility of the developed CRICED platform for 1 nM stDNA target (inset: visual images by CCD camera). (B) Effects of the incubation time of TSDR in the presence of stDNA target (1 nM). (C) Denaturing PAGE analysis of the activated Cas12a for cutting intDNA (200 nM). (D) CL value of the catalytic substrate as a function of time in the presence of stDNA target (0.1, 0.25, 0.5, 1 nM).

https://doi.org/10.1021/acs.analchem.2c01507
Anal. Chem. 2022, 94, 8506−8513

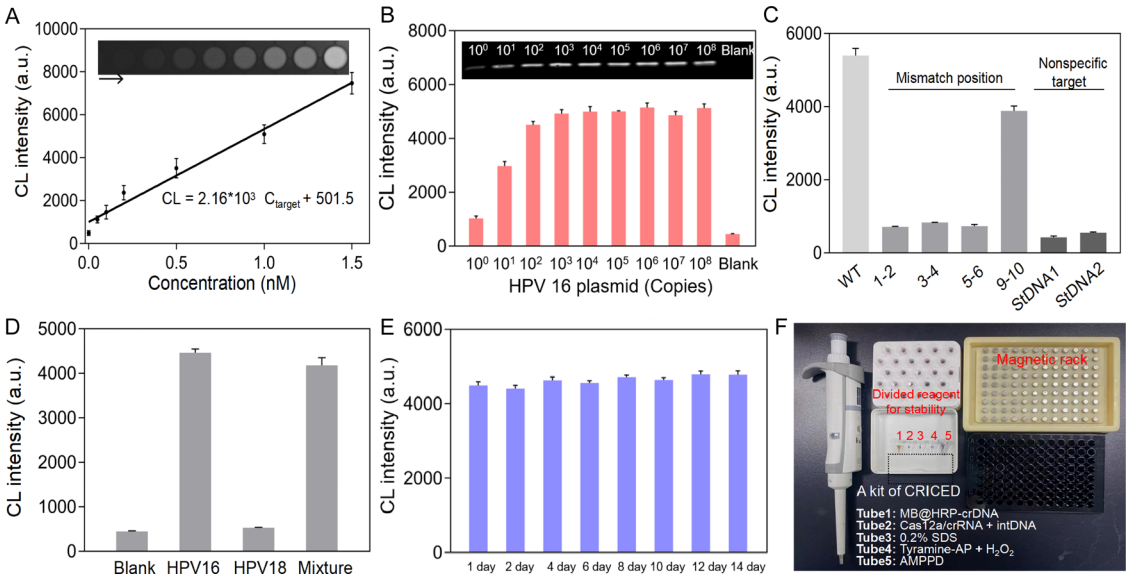

Figure 3. (A) Correlation curve for the relationship of the CL value vs the stDNA target concentration (0, 0.05, 0.10, 0.25, 0.50, 1.00, 1.50 nM) (inset: visual image changes of increasing concentration of stDNA target). (B) Evaluation of the detection sensitivity of the CRICED platform by combining RPA (inset: the amplified band from 10^0 to 10^8 copies). (C) Evaluation of the specificity of the CRICED platform using two base-mismatched targets and nonspecific targets by comparison to specific stDNA (1 nM). (D) Evaluation of the specificity of the CRICED platform using HPV18 plasmid (10^3 copies). (E) Stability evaluation of the CRICED platform. (F) Main laboratory equipment needed for the CRICED platform and partially packaged reagents for stability assay.

proposed strategy showed great potential for the detection of nucleic acids.

To achieve higher sensitivity, several experimental conditions like the concentrations of intDNA and Cas12a, incubation time of TSDR, and catalytic reaction time were optimized before its application in nucleic acid detection. The value of ΔCL was used to evaluate and appraise the performance of the proposed CRICED platform, where ΔCL represented the difference in the chemiluminescence intensity of the incubation solution in the presence and absence of the stDNA target. As the crDNA amounts coated on MB have a significant effect on the detection performance, the results in Figure S2A indicated that the CL value reached the maximum at 400 nM, indicating that 400 nM crDNA could completely cover the surface of MB. The influence of streptavidin−HRP concentration on the CL intensity was also investigated, and the highest CL value was captured at 1 μg/mL (Figure S2B). The concentration of intDNA plays a vital role during the TSDR event; it was found that the CL value gradually decreased accompanied by an increasing concentration of intDNA and showed a minimal value at 200 nM (Figure S2C). Meanwhile, the optimal incubation time of TSDR was determined to be 60 min (Figure 2B) under room temperature. According to the optimal concentration of intDNA, it is of great importance to explore the well-matched collateral activity of Cas12a. As seen in Figure 2C, 200 nM intDNA could be gradually cut into short bands along with the increasing concentration of Cas12a, and 200 nM Cas12a was the optimal concentration in the work. In addition, before being added to MB@HRP-crDNA, we had to destroy the activity of Cas12a in case of interference with the subsequent experiments. In general, the solution of SDS could irreversibly destroy the activity of proteins and was frequently applied to DNA hybridization solutions.[48] We found that the Cas12a was absolutely inactive after the addition of 0.2% SDS (Figure S2D). Furthermore, we moved to the response time of the catalytic substrate. As shown in Figure 2D, with different concentrations of intDNA in the range of 0.1 nM−1 nM, the maximum CL value appeared after 100 s, which was selected to be the best time point.

Analytical Performance of the CRICED Platform. Having ascertained the aforementioned experimental conditions, the analytical performance of our proposed CRICED was studied by a series of different concentrations of stDNA target. As shown in Figure 3A, the CL values increased accordingly with the increase of target concentrations, which was also consistent with imaging changes (Figure 3A, inset). Then, the correlation of the relative variation ratio with stDNA target concentration was studied. A good linearity could be obtained ranging from 0.05 to 1.5 nM (Figure 3A). The calculated detection limit was as low as 17 pM based on $3\sigma/S$, which was better than most of the previously reported methods (Table S2). We further attempted to explore the CRICED platform for the detection of HPV16 plasmid by combining an RPA kit, and the concentration of plasmid samples ranging from 10^0−10^8 copies were rapidly amplified for 30 min (Figure 3B, inset). The CRICED platform could detect as low as one copy per reaction of the HPV16 plasmid (Figure 3B).

We next challenged the CRICED platform by virtue of synthetic mismatched DNA targets (HPV16) and nonspecific targets (sequences are listed in Table S2). As shown in Figure 3C, the CL values of two base-pair mismatched targets located near the PAM area (from position 1 to position 6) critically affected the collateral cleavage activity of Cas12a, and positions 9−10 exhibited a weak inhibition effect; meanwhile, the nonspecific targets (stDNA1 and stDNA2) showed nearly no CL signals, which were consistent with a previous study of Cas12a.[6] Additionally, we evaluated the CRICED platform toward other HPV genotypes (HPV18) as an interfering substance. As shown in Figure 3D, the amplified HPV18 plasmid and blank group induced negligible changes in the CL signal, whereas the mixture was similar to that of the HPV16

https://doi.org/10.1021/acs.analchem.2c01507
Anal. Chem. 2022, 94, 8506−8513

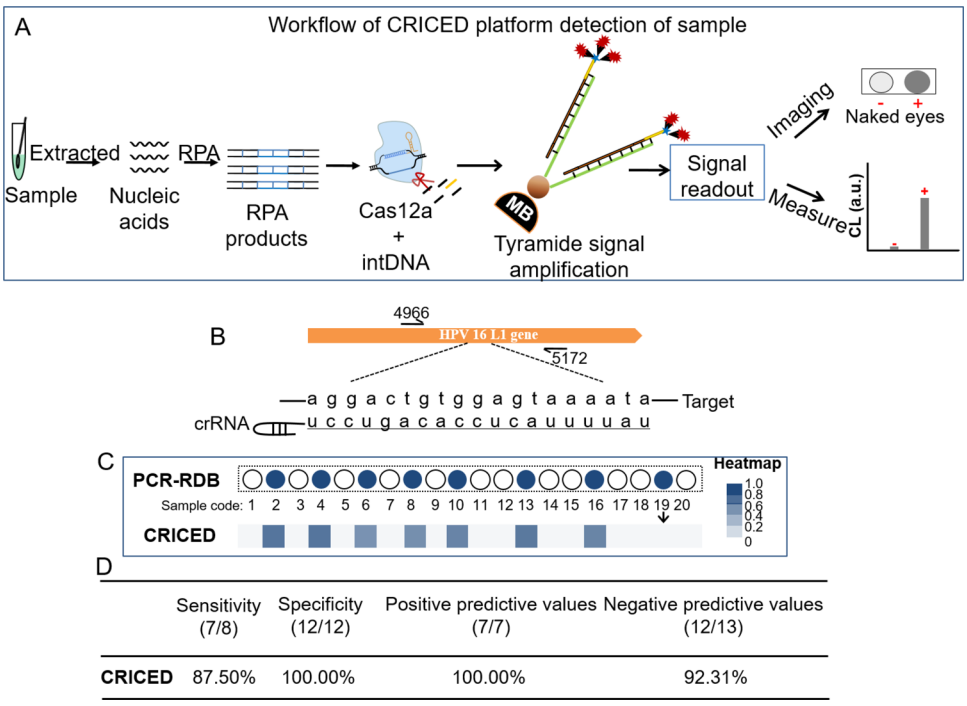

Figure 4. (A) Schematic diagram showing the workflow of the CECRID platform for the detection of clinical samples. (B) Schematic diagram of the full length of the L1 gene of the HPV16 genome and target gene sites for crRNA set and RPA primers sites. (C) Heatmap analysis of the CRICED platform vs PCR-RDB schematic results except for sample number 19 (HPV16), as shown by the black arrow. (D) Positive and negative predictive values, sensitivity, and specificity of CRICED for HPV16 clinical samples.

plasmid alone. Together, the CRICED platform demonstrated an excellent specificity for nucleic acid analysis.

To improve the simplicity and convenience of the CRICED platform, we divided the involved reagents into five tubes according to different experimental performances (Figure 3F, inset). We evaluated the stability of the proposed assay for consecutive 14 days. We mainly focused on the stability of as-obtained MB@HRP-crDNA; the CL value was measured daily using packaged reagents under the same stDNA target (1 nM) condition. Those results suggested that there was no obvious change in the CL response after 14 days of placement (Figure 3E). The proposed CRICED platform exhibited acceptable stability and laid the foundation for the development of CRISPR/Cas12a-based molecular diagnostic kits.

Clinical Application. With aforesaid optimized conditions, the whole process of the CRICED platform for the detection of clinical samples is summarized in Figure 4A; the extracted nucleic acids were quickly amplified with an RPA kit, and the RPA products were injected into the solution of Cas12a/crRNA and intDNA. The remarkable signal via the TSA strategy could be judged by measuring the CL value or visual readout. The high-risk HPV16 is the most prevalent genotype in HPV-associated cancers, including cervical cancer.[49,50] To validate the clinical performance of the CRICED platform, we designed the crRNA and RPA primer sites from the specific L1 gene of HPV16 (Figure 4B, sequences are listed in Table S2). We extracted crude DNA in cervical swabs collected from 20 HPV-infected patients in a clinical laboratory. We preferentially tested HPV samples with a commercial HPV genotyping kit for 23 types (PCR-RDB, reverse dot blot) and obtained 12 negative samples and eight positive samples of HPV16 (Figures S3 and S4). Those confirmed clinical samples were subsequently detected by the proposed CRICED platform (Figure S5), achieving highly consistent results in agreement with the results for 20 samples except for one sample (Figure 4C), with satisfying 100.00% positive predictive agreement and 92.31% negative predictive agreement (Figure 4D). Noteworthily, the CRICED platform also exhibited superior sensitivity (87.50%) and specificity (100.00%) with HPV clinical samples (Figure 4D). Taken together, these results highlight the application of the CECRID platform for nucleic acid diagnosis in real clinical samples.

CONCLUSIONS

In this work, we proposed a CRISPR/Cas12a-triggered chemiluminescence enhancement biosensor by recruiting a tyramide signal amplification strategy for the first time, achieving the ultrasensitive detection of nucleic acids in detectable signals or visual image readouts. The CRICED platform not only provides a high detection sensitivity of 17 pM and single copy per reaction for respective stDNA target and plasmid but also exhibits excellent specificity and stronger stability. More significantly, the proposed CRICED platform was evaluated to test 20 clinical HPV samples by comparison with the PCR-RDB gold standard method, showing superior sensitivity and specificity with patient samples. More to the point, we believe that the CRICED platform could be easily programmable for the detection of other pathogens, miRNA, and SNPs by designing specific crRNA(s). In particular, the ongoing COVID-19 pandemic has evolved into a worldwide public health crisis with significant mortality and morbidity.[51] We anticipate that our proposed CRICED platform could become a promising alternative method in terms of SARS-CoV-2 or other pathogen detection and build preparedness for potential infectious disease outbreaks. Overall, we envisage that our remarkably ultrasensitive and specific CRICED platform

https://doi.org/10.1021/acs.analchem.2c01507
Anal. Chem. 2022, 94, 8506−8513

paves the way for developing a robust test kit for practical application of CRISPR-based detection technology.

■ ASSOCIATED CONTENT

Supporting Information

The Supporting Information is available free of charge at https://pubs.acs.org/doi/10.1021/acs.analchem.2c01507.

The procedure of MB@AP-crDNA preparation; PAGE analysis procedure; CL characterization of MB@AP-crDNA and MB@AP-crDNA with the TSA strategy; optimization of experimental conditions of the CRICED platform; HPV clinical sample results by PCR-RDB; and CL values of HPV clinical samples by the CRICED platform (PDF)

■ AUTHOR INFORMATION

Corresponding Author

Tao Hu − *The Children's Hospital, Zhejiang University School of Medicine, National Clinical Research Center for Child Health, Hangzhou, Zhejiang 310052, China;* orcid.org/0000-0003-3448-6515; Email: hutaozd@zju.edu.cn; Fax: +86 571 86670488

Authors

Xinxin Ke − *The Children's Hospital, Zhejiang University School of Medicine, National Clinical Research Center for Child Health, Hangzhou, Zhejiang 310052, China*

Yangjing Ou − *International Peace Maternity & Child Health Hospital, Shanghai Municipal Key Clinical Specialty, Institute of Embryo-Fetal Original Adult Disease, School of Medicine, Shanghai Jiao Tong University, Shanghai 200030, China*

Yu Lin − *International Peace Maternity & Child Health Hospital, Shanghai Municipal Key Clinical Specialty, Institute of Embryo-Fetal Original Adult Disease, School of Medicine, Shanghai Jiao Tong University, Shanghai 200030, China*

Complete contact information is available at: https://pubs.acs.org/10.1021/acs.analchem.2c01507

Author Contributions

The manuscript was written through contributions of all authors.

Notes

The authors declare no competing financial interest.

■ ACKNOWLEDGMENTS

This work was supported by the National Natural Science Foundation of China (81901536) and Project of Children's Hospital Affiliated with Zhejiang University School of Medicine (Y021026).

■ REFERENCES

(1) Yang, M.; Liu, Y.; Jiang, X. *Chem. Soc. Rev.* **2019**, *48*, 850−884.
(2) Yang, Y.; Chen, Y.; Tang, H.; Zong, N.; Jiang, X. *Small Methods* **2020**, *4*, No. 1900451.
(3) Urdea, M.; Penny, L.; Olmsted, S.; Giovanni, M.; Kaspar, P.; Shepherd, A.; Wilson, P.; Dahl, C.; Buchsbaum, S.; Moeller, G.; Deborah, C.; Hay Burgess, D. *Nature* **2006**, *444*, 73−79.
(4) Horvath, P.; Barrangou, R. *Science* **2010**, *327*, 167−170.
(5) Feng, W.; Newbigging, A.; Tao, J.; Cao, Y.; Peng, H.; Le, C.; Wu, J.; Pang, B.; Li, J.; Tyrrell, D.; Zhang, H.; Le, X. *Chem. Sci.* **2021**, *12*, 4683−4698.
(6) Chen, J. S.; Ma, E.; Harrington, L. B.; Da Costa, M.; Tian, X.; Palefsky, J. M.; Doudna, J. A. *Science* **2018**, *360*, 436−439.
(7) Gootenberg, J.; Abudayyeh, O.; Lee, J.; Ess-letzbichler, P.; Dy, A.; Joung, J.; Verdine, V.; Donghia, N.; Daringer, N.; Freije, C.; Myhrvold, C.; Bhattacharyya, R.; Livny, J.; Regev, A.; Koonin, E.; Hung, D.; Sabeti, P.; Collins, J.; Zhang, F. *Science* **2017**, *356*, 438−442.
(8) Teng, F.; Guo, L.; Cui, T.; Wang, X.; Xu, K.; Gao, Q.; Zhou, Q.; Li, W. *Genome Biol.* **2019**, *20*, No. 132.
(9) Harrington, L.; Burstein, D.; Chen, J.; Paez-Espino, D.; Ma, E.; Witte, I.; Cofsky, J.; Kyrpides, N.; Banfield, J.; Doudna, J. *Science* **2018**, *362*, 839−842.
(10) Pickar-Oliver, A.; Gersbach, C. *Nat. Rev. Mol. Cell. Biol.* **2019**, *20*, 490−507.
(11) Ackerman, C. M.; Myhrvold, C.; Thakku, S.; Freije, C.; Metsky, H.; Yang, D.; Ye, S.; Boehm, C.; Kosoko-Thoroddsen, T.; Kehe, J.; Nguyen, T.; Carter, A.; Kulesa, A.; Barnes, J.; Dugan, V.; Hung, D.; Blainey, P.; Sabeti, P. *Nature* **2020**, *582*, 277−282.
(12) Ramachandran, A.; Santiago, J. G. *Anal. Chem.* **2021**, *93*, 7456−7464.
(13) Nouri, R.; Tang, Z.; Dong, M.; Liu, T.; Kshir-sagar, A.; Guan, W. *Biosens. Bioelectron.* **2021**, *178*, No. 113012.
(14) Li, L.; Li, S.; Wu, N.; Wu, J.; Wang, G.; Zhao, G.; Wang, J. *ACS. Synth. Biol.* **2019**, *8*, 2228−2237.
(15) Drobysh, M.; Ramanaviciene, A.; Viter, R.; Chen, C.; Samukaite-Bubniene, U.; Ratautaite, V.; Ramanavicius, A. *Int. J. Mol. Sci.* **2022**, *23*, 666.
(16) Smith, C.; Nandu, N.; Kachwala, M.; Chen, Y.; Uyar, T.; Yigit, M. *Biochemistry* **2020**, *59*, 1474−1481.
(17) Dronina, J.; Samukaite-Bubniene, U.; Ramanavicius, A. *J. Nanobiotechnology* **2022**, *20*, No. 41.
(18) Yin, L.; Man, S.; Ye, S.; Liu, G.; Ma, L. *Biosens. Bioelectron.* **2021**, *193*, No. 113541.
(19) Zhang, Y.; Chen, M.; Liu, C.; Chen, J.; Luo, X.; Xue, Y.; Liang, Q.; Zhou, L.; Tao, Y.; Li, M.; Wang, D.; Zhou, J.; Wang, J. *Sens. Actuators, B* **2021**, *345*, No. 130411.
(20) Jiang, Y.; Hu, M.; Liu, A.; Lin, Y.; Liu, L.; Yu, B.; Zhou, X.; Pang, D. W. *ACS Sens.* **2021**, *6*, 1086−1093.
(21) Hu, M.; Yuan, C.; Tian, T.; Wang, X.; Sun, J.; Xiong, E.; Zhou, X. *J. Am. Chem. Soc.* **2020**, *142*, 7506−7513.
(22) Mukama, O.; Wu, J.; Li, Z.; Liang, Q.; Yi, Z.; Lu, X.; Liu, Y.; Liu, Y.; Hussain, M.; Makafe, G.; Liu, J.; Xu, N.; Zeng, L. *Biosens. Bioelectron.* **2020**, *159*, No. 112143.
(23) Dai, Y.; Somoza, R.; Wang, L.; Welter, J.; Li, Y.; Caplan, A.; Liu, C. *Angew. Chem., Int. Ed.* **2019**, *58*, 17399−17405.
(24) Ge, H.; Wang, X.; Xu, J.; Lin, H.; Zhou, H.; Hao, T.; Wu, Y.; Guo, Z. *Anal. Chem.* **2021**, *93*, 14885−14891.
(25) Wang, Q.; Liu, Y.; Yan, J.; Liu, Y.; Gao, C.; Ge, S.; Yu, J. *Anal. Chem.* **2021**, *93*, 13373−13381.
(26) Zhang, K.; Fan, Z.; Huang, Y.; Ding, Y.; Xie, M. *Talanta* **2022**, *236*, No. 122868.
(27) Liu, S.; Wang, C.; Wang, Z.; Xiang, K.; Zhang, Y.; Fan, G.; Zhao, L.; Han, H.; Wang, W. *Biosens. Bioelectron.* **2022**, *204*, No. 114078.
(28) Yahyai, I.; Lawati, H. *Luminescence* **2021**, *36*, 266−277.
(29) Yang, M.; Huang, J.; Fan, J.; Du, J.; Pu, K.; Peng, X. *Chem. Soc. Rev.* **2020**, *49*, 6800−6815.
(30) Xu, L.; Cao, Z.; Ma, R.; Wang, Z.; Qin, Q.; Liu, E.; Su, B. *Anal. Chem.* **2019**, *91*, 12859−12865.
(31) Kricka, L. *Anal. Chim. Acta* **2003**, *500*, 279−286.
(32) Speletas, M.; Kyritsi, M.; Vontas, A.; The-odoridou, A.; Chrysanthidis, T.; Hatzianastasiou, S.; Petinaki, E.; Hadjichristodoulou, C. *Front. Immunol.* **2020**, *11*, No. 609242.
(33) Mei, S.; Liu, B.; Xiong, X.; Hun, X. *J. Pharm. Biomed. Anal.* **2020**, *186*, No. 113280.
(34) Hatakeyama, K.; Tanaka, T.; Sawaguchi, M.; Iwadate, A.; Mizutani, Y.; Sasaki, K.; Tateishi, N.; Matsunaga, T. *Lab Chip* **2009**, *9*, 1052−1058.

(35) Yao, Y.; Wang, X.; Duan, W.; Li, F. *Analyst* **2018**, *143*, 709−714.
(36) Li, Y.; Sun, L.; Zhao, Q. *Anal. Chem.* **2019**, *91*, 2615−2619.
(37) Xiao, Q.; Wu, J.; Dang, P.; Ju, H. *Anal. Chim. Acta* **2018**, *1032*, 130−137.
(38) Stack, E.; Wang, C.; Roman, K.; Hoyt, C. *Methods* **2014**, *70*, 46−58.
(39) Fominaya, A.; Loarce, Y.; González, J.; Ferrer, E. *Plant Cytogenetics. Methods in Molecular Biology*; Humana Press, 2016; Vol. *1429*, pp 35−48.
(40) Huang, Z.; Lin, Q.; Yang, B.; Ye, X.; Chen, H.; Weng, W.; Kong, J. *Chem. Commun.* **2020**, *56*, 12793−12796.
(41) Yuan, L.; Xu, L.; Liu, S. *Anal. Chem.* **2012**, *84*, 10737−10744.
(42) Chen, Y.; Zhang, S.; Hong, Z.; Lin, Y.; Dai, H. *J. Mater. Chem. B.* **2019**, *7*, 6972−6980.
(43) Zhao, L.; Fu, Y.; Ren, S.; Cao, J.; Liu, Y. *Biosens. Bioelectron.* **2021**, *171*, No. 112729.
(44) Zong, C.; Jiang, F.; Wang, X.; Li, P.; Xu, L.; Yang, H. *Biosens. Bioelectron.* **2021**, *177*, No. 112998.
(45) Liu, P.; Li, C.; Zhang, R.; Tang, Q.; Wei, J.; Lu, Y.; Shen, P. *Biosens. Bioelectron.* **2019**, *126*, 543−550.
(46) Dai, W.; Dong, H.; Guo, K.; Zhang, X. *Chem. Sci.* **2017**, *9*, 1753−1759.
(47) Wu, H.; Liu, Y.; Li, M.; Chong, Y.; Zeng, M.; Lo, Y.; Yin, J. *Nanoscale* **2015**, *7*, 4505−4513.
(48) Li, S.; Peng, Q.; Liao, S.; Li, W.; Ma, Q.; Lu, X. *PLoS. One* **2017**, *12*, No. e0177196.
(49) Ho, N.; Lim, G.; Sundah, N.; Lim, D.; Loh, T.; Shao, H. *Nat. Commun.* **2018**, *9*, No. 3238.
(50) Malagón, T.; Louvanto, K.; Wissing, M.; Burchell, A.; Tellier, P.; El-Zein, M.; Coutlée, F.; Franco, E. *Lancet Infect. Dis.* **2019**, *19*, 317−326.
(51) Ratautaite, V.; Boguzaite, R.; Brazys, E.; Ramanaviciene, A.; Ciplys, E.; Juozapaitis, M.; Slibinskas, R.; Bechelany, M.; Ramanavicius, A. *Electrochim. Acta* **2022**, *403*, No. 139581.

https://doi.org/10.1021/acs.analchem.2c01507
Anal. Chem. 2022, 94, 8506−8513